A Global Low Order Spectral Model Designed for Climate Sensitivity Studies

Adel F. Hanna and Duane E. Stevens

DEPARTMENT OF ATMOSPHERIC SCIENCE

COLORADO STATE UNIVERSITY

FORT COLLINS, COLORADO

A GLOBAL LOW ORDER SPECTRAL MODEL DESIGNED

FOR CLIMATE SENSITIVITY STUDIES

Adel F. Hanna
and
Duane E. Stevens

Department of Atmospheric Science
Colorado State University
Fort Collins, Colorado   80523

March 1984

Atmospheric Science Paper No. 378

Abstract

A two-level, global, spectral model using pressure as a vertical coordinate is developed. The system of equations describing the model is nonlinear and quasi-geostrophic (linear balance) (Lorenz, 1960). A moisture budget is calculated in the lower layer only with moist convective adjustment between the two layers. The mechanical forcing of topography is introduced as a lower boundary vertical velocity. Solar forcing is specified assuming a daily mean zenith angle. On land and sea ice surfaces a steady state thermal energy equation is solved to calculate the surface temperature. Over the oceans the sea surface temperatures are prescribed from the climatological average of January. The model is integrated to simulate the January climate.

Acknowledgments

Table of Contents

LIST OF FIGURES

LIST OF SYMBOLS

a	radius of the earth
a_0, a_1, a_2 and a_3	longwave radiation constants
a_m	mean distance between the earth and the sun
a_s	instantaneous distance between the earth and the sun
AP	available potential energy
$(AP)_n^m$	spherical harmonic mode of AP
$b_{oo}, \ldots b_{23}$	longwave radiation constants
B	Stefan-Boltzmann constant
B_a	the net heating of the atmosphere
B_s	the net surface heating
B_{ea}	the net heating of the earth-atmosphere system
c	fractional amount of low and medium clouds (tenths)
c_d	surface drag coefficient
c_p	specific heat at constant pressure
D_n^m	$D_n^m = (n^2 - m^2/4n^2 - 1)^{\frac{1}{2}}$
E	evaporation rate
f	the Coriolis parameter
F_h	rate of change of vorticity due to horizontal diffusion
F_v	rate of change of vorticity due to vertical diffusion
GW	wetness parameter
h_s	relative humidity near the surface
H_o	hour angle of the sun
i	$i = \sqrt{-1}$

vi

I	thermal conductivity of ice per unit length
I_s	number of Gaussian latitudes used in the transform method
J	highest wave number of $n-m$ retained in the truncated series, or Jacobian
k	vertical unit vector
k_d	friction coefficient
k_h	lateral eddy diffusion coefficient
k_s	surface friction coefficient
KE	kinetic energy
$(KE)_n^m$	spherical harmonic mode of KE
ℓ	index of the vertical level
L	latent heat of condensation,
L_o	net longwave radiation at the surface
L_4	net longwave flux at the top of the atmosphere
m	zonal wave number
M	highest zonal wave number retained in the truncated series
n	degree of a spherical harmonic component
N	number of days measured from day 0 to 00Z 1 January
N_g	number of grid points used in an integration around a latitude circle
N_s	net radiation at the surface
N_∞	net radiation at the top of the atmosphere
p	pressure
P_c	precipitation rate
P_g	pressure at the terrain height
P_n^m	associated Legendre functions of the first kind
q	moisture mixing ratio

q_s	saturation mixing ratio
Q	rate of heating per unit mass
Q_s	surface sensible heat flux
r	stress due to vertical diffusion
r_a	atmospheric albedo
r_s	surface albedo
R	gas constant for dry air
R_v	gas constant for water vapor
S_c	solar constant
S_h	rate of change of mixing ratio due to horizontal diffusion
S_r	solar radiation absorbed by the atmosphere
S_s	solar radiation absorbed by the earth's surface
S_∞	incident solar radiation at the top of the atmosphere
t	time
T	air temperature
T_a	air temperature at 1000 mb
T_c	thermal conductivity of ice
T_g	surface ground temperature
u	zonal wind speed
v	meridional wind speed
$\underline{v}$	horizontal wind vector
$\underline{v}_o$	rotational part of the horizontal wind vector at level 1
W_h	rate of change of potential temperature due to horizontal diffusion
W_v	rate of change of potential temperature due to vertical diffusion
x	absorptivity of the atmosphere
X	a general parameter

X_n^m	spherical harmonic coefficient of X
y	longwave effective emissivity at the surface
Y_n^m	spherical harmonic
$\bar{z}$	daily average zenith angle
α	radiation constant
β	radiation constant
γ	critical relative humidity in the lower layer
Γ	temperature lapse rate
Γ_s	moist adiabatic lapse rate
δ	declination angle
ε_g	longwave emissivity at the surface
ζ	vorticity
θ	potential temperature
θ_n^m	spherical harmonic coefficient of θ
κ	$\kappa = R/c_p$
λ	geographic longitude
μ	$\mu = \sin(\phi)$
ν	iteration index
π	$\pi = 3.141593$
ρ	density of air
ρ_s	density of air near the surface
σ	static stability
σ_n^m	spherical harmonic coefficient of σ
τ	rotational shear between the two levels
θ_n^m	spherical harmonic coefficient of τ
ϕ	geographic latitude
χ	velocity potential

χ_0	surface velocity potential
χ_n^m	spherical harmonic coefficient of χ
$(\chi_0)_n^m$	spherical harmonic coefficient of χ_0
ψ	stream function
ψ_0	surface stream function
ψ_n^m	spherical harmonic coefficient of ψ
$(\psi_0)_n^m$	spherical harmonic coefficient of ψ_0
ω	vertical pressure velocity
Ω	angular velocity of rotation of the earth
∇	horizontal del-operator $\nabla \equiv (\partial/a\cos\phi\ \partial\lambda,\ 1/a\partial\phi)$
$()^*$	the asterisk $*$ denotes the complex conjugate, or
	departure from the time average
$\|\ \|$	absolute value

1. Introduction

Numerical models are an important tool for testing many hypotheses concerning climate variability. During recent years a wide variety of models have been developed. Complexity of such models ranges between the simple energy balance models (e.g. Budyko, 1969; Sellers, 1973) and the multi-level primitive equation models (e.g. Manabe et al., 1965; Kasahara and Washington, 1971; Corby et al., 1977; Otto-Bleisner et al., 1982).

Intermediate complexity models (Kikuchi, 1969; Salmon and Hendershott, 1976; Held and Suarez, 1978), with reasonable dynamical and physical simplifications, can simulate some aspects of the largest scales of atmospheric motion. The computational economy of such models provides the opportunity for longer periods of simulation and for more extensive testing of physical and dynamical processes. Moreover, such models can provide a first insight on atmospheric problems before using the complicated general circulation models. Also, intermediate complexity models are useful for interpreting the results of more complicated models (Chervin, et al., 1980).

In this study a two-level spectral model using pressure as a vertical coordinate is developed. The system of equations describing the model is quasi-geostrophic in linear balance (Lorenz, 1960). The choice of global rather than hemispheric model is due to the fact that the latter is believed to excite anomalous Rossby waves (Roads and Somerville, 1982) which could be critical when dealing with climate sensitivity studies.

The physical forcing is parameterized with reasonable simplicity to include the major forcing mechanisms which develop the large scale

atmospheric circulation. The solar energy is specified as a function of latitude and time assuming a daily mean zenith angle (Wetherald and Manabe, 1972). The amount of solar energy absorbed by the model's atmosphere and the earth's surface is calculated using a formula given by Kubota (1972). Longwave radiation forcing of the two layers and the surface are calculated using climatological relative humidity and surface temperature. The mechanical forcing of topography is introduced in the form of a lower boundary vertical velocity. The differential diabatic heating due to the distribution of land and sea also is included. The sea surface temperatures are specified using the observed January mean values. On continents and ice surfaces the thermal energy balance equation is solved for the surface temperature.

$$4 \quad \underline{\hspace{2cm} \omega_4 = 0 \hspace{2cm}} \quad 0 \text{ mb}$$

$$3 \quad \underline{\hspace{2cm} \psi_3,\ \chi_3,\ \theta_3 \hspace{2cm}} \quad 250 \text{ mb}$$

$$2 \quad \underline{\hspace{2cm} \omega_2 \hspace{2cm}} \quad 500 \text{ mb}$$

$$1 \quad \underline{\hspace{2cm} \psi_1,\ \chi_1,\ \theta_1,\ q \hspace{2cm}} \quad 750 \text{ mb}$$

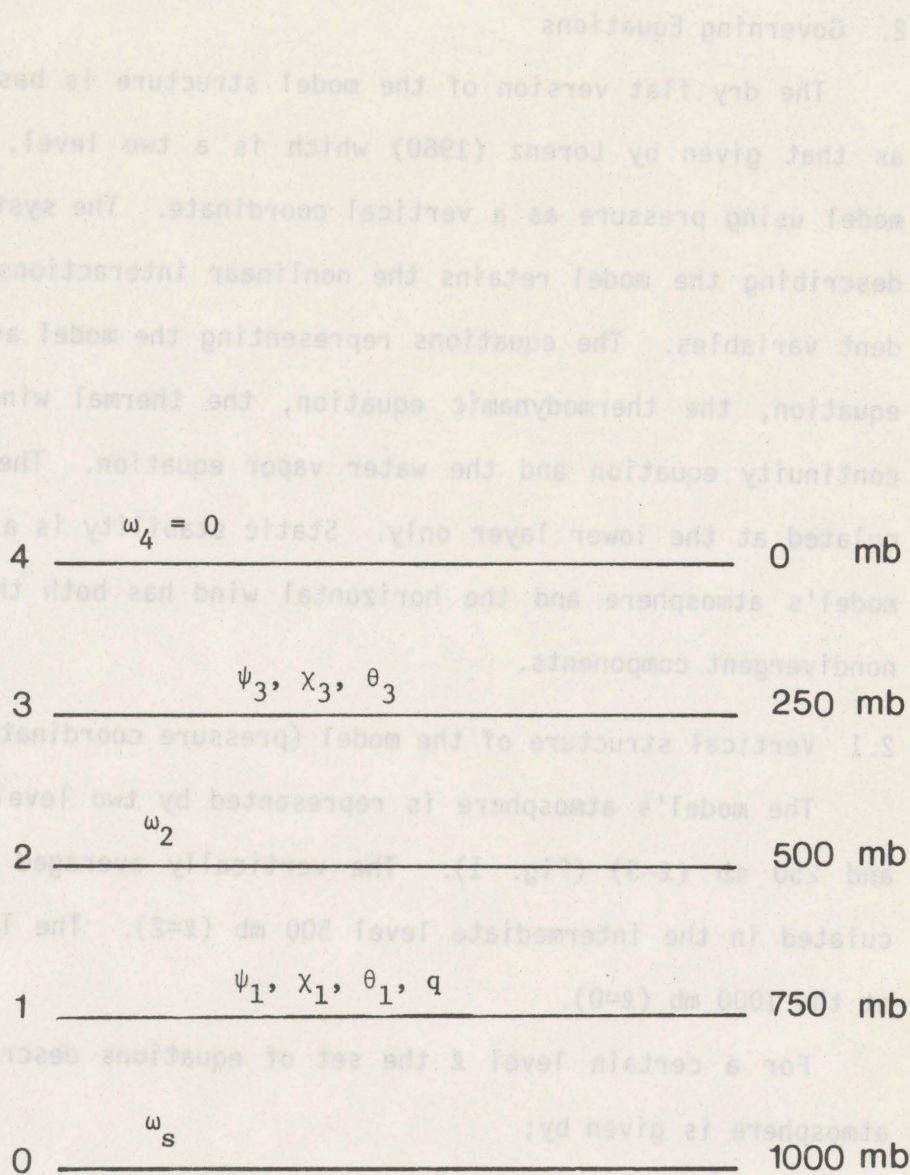$$0 \quad \underline{\hspace{2cm} \omega_s \hspace{2cm}} \quad 1000 \text{ mb}$$

Fig. 1. Schematic representation of the vertical structure of the model.

2. Governing Equations

The dry flat version of the model structure is basically the same as that given by Lorenz (1960) which is a two level, linear balance model using pressure as a vertical coordinate. The system of equations describing the model retains the nonlinear interactions between dependent variables. The equations representing the model are the vorticity equation, the thermodynamic equation, the thermal wind equation, the continuity equation and the water vapor equation. The latter is calculated at the lower layer only. Static stability is a variable in the model's atmosphere and the horizontal wind has both the divergent and nondivergent components.

2.1 Vertical structure of the model (pressure coordinate)

The model's atmosphere is represented by two levels; 750 mb ($\ell=1$) and 250 mb ($\ell=3$) (Fig. 1). The vertically averaged values are calculated in the intermediate level 500 mb ($\ell=2$). The lower boundary is at the 1000 mb ($\ell=0$).

For a certain level ℓ the set of equations describing the models atmosphere is given by;

$$\underline{v}_\ell = k \times \nabla\psi_\ell + \nabla\chi_\ell, \tag{2.1}$$

the vorticity equation

$$\frac{\partial}{\partial t} \nabla^2\psi_\ell = -J(\psi_\ell, \nabla^2\psi_\ell+f) - \nabla\chi_\ell \cdot \nabla f + f \frac{\partial\omega_\ell}{\partial p} + (F_h)_\ell + (F_v)_\ell, \tag{2.2}$$

the thermodynamic energy equation

$$\frac{\partial\theta_\ell}{\partial t} = -J(\psi_\ell,\theta_\ell) - \nabla\chi_\ell \cdot \nabla\theta_\ell - \omega_\ell \frac{\partial\theta_\ell}{\partial p} + \left(\frac{p_0}{p_\ell}\right)^\kappa \frac{Q_\ell}{c_p} + (W_h)_\ell + (W_v)_\ell, \tag{2.3}$$

the thermal wind equation

$$c_p(p_0)^{-\kappa} \nabla^2 \theta_\ell = -\nabla \cdot \frac{\partial}{\partial p^\kappa} (f \nabla \psi_\ell),$$ (2.4)

the continuity equation

$$\frac{\partial \omega_\ell}{\partial p} + \nabla^2 \chi_\ell = 0,$$ (2.5)

and the water vapor equation

$$\frac{\partial q}{\partial t} = -\nabla \cdot (\underline{v}_1 q) + E - P_c + (S_h)_1.$$ (2.6)

where $\underline{v}_\ell = (u_\ell, v_\ell)$ is the horizontal wind vector, ω_ℓ the vertical pressure velocity, f is the coriolis parameter, ψ_ℓ is the stream function, χ_ℓ is the velocity potential, θ_ℓ is the potential temperature, q is the water vapor mixing ratio, p_ℓ is the pressure, p_0 is the lower boundary pressure level ($\equiv$ 1000 mb), P_c is the precipitation rate, E is the surface evaporation rate, Q_ℓ/c_p is the diabatic heating rate, c_p is the specific heat at constant pressure, $\kappa = R/c_p$, R is the gas constant, F_h, W_h, S_h are the horizontal diffusion of momentum, heat and moisture respectively, $(F_v)_\ell$ and $(W_v)_\ell$ are the vertical diffusion of momentum and heat, respectively.

Equations (2.1)-(2.6) are six equations in the 14 unknowns ψ_ℓ, χ_ℓ, θ_ℓ, ω_ℓ, q, $\underline{v}_\ell$, Q_ℓ, $(F_h)_\ell$, $(F_v)_\ell$, $(W_h)_\ell$, $(W_v)_\ell$, $(S_h)_1$, E and P_c. The evaporation rate, E, is a result of the moisture vertical diffusion from the surface while, the precipitation P_c is calculated as the excess of super saturated moisture in the lower layer. In order to close the set (2.1)-(2.6) the diabatic heating and the diffusion terms need to be parameterized in terms of the dependent variables.

2.2 Horizontal diffusion

From the numerical stability view point the diffusive terms are not required when using the spectral method. There is a requirement to inhibit spurious growth of amplitude at scales close to the point of truncation due to spectral blocking (Puri and Bourke, 1974). At a level ℓ the horizontal diffusion of momentum, heat and moisture is parameterized, respectively.

$$(F_h)_\ell = k_h \, \nabla^2 \, (\nabla^2 \psi_\ell + 2 \, \frac{\psi_\ell}{a^2}), \qquad (2.7)$$

$$(W_h)_\ell = k_h \, \nabla^2 \theta_\ell, \qquad (2.8)$$

$$(S_h)_\ell = k_h \, \nabla^2 q, \qquad (2.9)$$

where k_h is the lateral eddy diffusion coefficient. The value of k_h is taken to be $1.0 \times 10^{+5}$ m^{2}sec^{-1} (Phillips, 1956). The last term to the right side of (2.7) is due to the effect of spherical earth.

2.3 Vertical diffusion

The planetary boundary layer is a transition layer in the atmosphere which separates between the earth surface and the large scale atmospheric motions. In this layer, which is approximately 1 km, the fluxes are mainly a consequence of small-scale turbulence and convection. In a large scale model it is necessary to utilize the effects of the boundary layer to simulate a correct phase and amplitude of the ultra-long waves. Parameterized bulk formulas are used here to calculate the friction dissipation, sensible heat flux and evaporation rate.

2.3.1 Parameterization of frictional dissipation

The two assumptions used for parameterizing the frictional dissipa-tion are as follows (Lorenz, 1961):

a) Surface frictional drag is proportional to the flow in the surface layer,

b) Friction between the two layers is proportional to the dif-ference between the flow of the two layers.

The friction dissipation, $(F_v)_\ell$, is given by

$$(F_v)_\ell = - g \frac{\partial r_\ell}{\partial p},$$ (2.10)

where g is the acceleration of gravity and r_ℓ is the rotational stress at level ℓ.

Using the above two assumptions we can have

$$r_0 = \frac{\Delta p}{g} k_s \nabla^2 \psi_0,$$ (2.11)

and

$$r_2 = \frac{\Delta p}{g} 2k_d \nabla^2(\psi_3 - \psi_1),$$ (2.12)

where $\Delta p(=p_0/2)$ is the pressure difference between the upper and lower levels, and ψ_0 is the surface stream function calcualted by linear extrapolation with respect to height (Salmon and Hendershott, 1976). k_s and $2k_d$ are the coefficients of friction at the underlying surface and the surface separating the two layers respectively. k_s is given the value $4\times10^{-6} \sec^{-1}$ (Kikuchi, 1969), and k_d is given the value $5\times10^{-7} \sec^{-1}$ (Charney, 1959).

Using (2.10), (2.11) and (2.12), and assuming that r_4 at the top of the atmosphere is equal to zero, we can find the expressions for the friction dissipation at the two levels,

$$(F_v)_1 = - k_s \nabla^2 \psi_0 + 2k_d \nabla^2 (\psi_3 - \psi_1), \tag{2.13}$$

$$(F_v)_3 = - 2k_d \nabla^2 (\psi_3 - \psi_1), \tag{2.14}$$

2.3.2 Parameterization of sensible heat

Over all surfaces, whether bare land, ice or water, the vertical (turbulent) flux of sensible heat Q_s is determined using the parameterization

$$Q_s = \rho_s c_p c_d |v_o| (T_g - T_a), \tag{2.15}$$

where ρ_s is the surface air density, T_g is the ground or surface temperature (prescribed over the oceans), T_a the surface air temperature, c_d is the drag coefficient and $|v_o|$ is the absolute value of the surface wind.

The surface air temperature, T_a, is extrapolated from the temperature values at 250 mb and 750 mb with respect to logarithm of the pressure level,

$$(T_a - T_1)/(T_a - T_3) = \ell n(p_0/p_1)/\ell n(p_0/p_3) \cong .207 \tag{2.16}$$

The drag coefficient, c_d, is assumed constant taken to be .004 and .001 over land and water surfaces respectively. By assuming these constant values for the drag coefficient we neglected its possible variations with the surface wind speed and the terrain height. The absolute value of the surface wind, $|v_o|$, is taken from the rotational part of the 750 mb wind. A minimum value is specified by 3 m sec^{-1} to avoid unrealistic high surface temperatures (Holloway and Manabe, 1971).

2.3.3 Parameterization of surface evaporation rate

The surface evaporation rate, E, is parameterized in the model as

$$E = \rho_s \, c_d \, |v_o| \, GW \, (h_* q_s(T_g) - h_s \, q_s(T_a)), \qquad (2.17)$$

where $q_s(T_g)$ is the saturation mixing ratio using the surface tempera-
ture, $q_s(T_a)$ the saturation mixing ratio at 1000 mb. The saturation
vapor pressure is calculated using a formula given by Bolton (1980).
The ground wetness parameter GW is a nondimensional measure of the
surface water available for evaporation and varies between 0 and 1.
Over water and ice it is taken as unity, whereas over land surfaces it
is taken as .25. The relative humidity in the atmosphere near the
surface, h_s, is given by $h_s = .5 \, q(T_1)/q_s(T_1)+.5$, where $q(T_1)$ is the
mixing ratio in the lower layer. h_* is simply set equal to 1; the
surface is assumed to be everywhere saturated (the "swamp" lower boun-
dary condition).

2.4 Mechanical forcing of topography

At the top of the model's atmosphere (p=0) the vertical pressure
velocity ω_4 is taken to be zero. At the lower boundary (1000 mb) ω_0
introduce the mechanical effect of topography, the kinematic condition

$$\omega_0 = J(\psi_1, P_g), \qquad (2.18)$$

is used. Here P_g is the pressure at the terrain height. When computing
P_g, the continental elevations smoothed over 5° latitude by 5° longitude
are used (Berkofsky and Berton, 1955) assuming a standard atmosphere.
In this relation the advection by the divergent part of the horizontal
wind is ignored.

Integration of the continuity equation (2.5) over the depth of the
model's atmosphere and through its two layers gives the following pres-
sure velocities

$$\omega_0 = -\Delta p \nabla^2 (\chi_1 + \chi_3), \tag{2.19}$$

$$\omega_1 = -\frac{\Delta p}{2} \nabla^2 (2\chi_3 + \chi_1), \tag{2.20}$$

and

$$\omega_3 = -\frac{\Delta p}{2} \nabla^2 (\chi_3). \tag{2.21}$$

It is convenient to introduce the new variable χ_0 such that

$$\omega_0 = -\Delta p \nabla^2 \chi_0. \tag{2.22}$$

From (2.19) and (2.22) we get

$$\chi_0 = \chi_1 + \chi_3 \tag{2.23}$$

The low order truncation used in the model (truncate at either zonal wave number 9 or wave number 15) is considered as a further filter to satisfy the quasi-geostrophic approximation, where the vertical velocity should be three orders of magnitude less than the horizontal wind (Haltiner, 1971).

2.5 The model

It is convenient to use as dependent variables the mean potential temperature θ and the static stability σ, the stream functions ψ and τ for the mean wind and wind shear, so that $\theta_3 = \theta + \sigma$, $\theta_1 = \theta - \sigma$, $\psi_3 = \psi + \tau$, $\psi_1 = \psi - \tau$, $\chi_1 = \chi$. Using (2.7) - (2.9), (2.13) and (2.14), the governing equations (2.1) - (2.6) become

$$\frac{\partial}{\partial t}(\nabla^2 \psi) = -J(\psi, \nabla^2 \psi + f) - J(\tau, \nabla^2 \tau) - \tfrac{1}{2} \nabla \cdot (f \nabla \chi_0) - \frac{k_s}{2} \nabla^2 \psi_0 + k_h (\nabla^4 \psi + 2\frac{\nabla^2 \psi}{a^2}), \tag{2.24}$$

$$\frac{\partial}{\partial t}(\nabla^2\tau) = -J(\psi,\nabla^2\tau)-J(\tau,\nabla^2\psi+f)+\nabla\cdot(f\nabla\chi)-\tfrac{1}{2}\nabla\cdot(f\nabla\chi_0)+\frac{k_s}{2}\nabla^2\psi_0-2k_d\nabla^2\tau$$

$$+ k_h(\nabla^4\tau + \frac{2}{a^2}\nabla^2\tau), \tag{2.25}$$

$$\frac{\partial\theta}{\partial t} = -J(\psi,\theta)-J(\tau,\sigma)+\nabla\cdot(\sigma\nabla\chi)-\tfrac{1}{2}(\nabla\chi_0\cdot\nabla\theta+\nabla\chi_0\cdot\nabla\sigma+3\sigma\nabla^2\chi_0)+k_h\nabla^2\theta+\bar{Q}, \tag{2.26}$$

$$\frac{\partial\sigma}{\partial t} = -J(\psi,\sigma)-J(\tau,\theta)+\nabla\chi\cdot\nabla\theta-\tfrac{1}{2}(\nabla\chi_0\cdot\nabla\theta+\nabla\chi_0\cdot\nabla\sigma-\sigma\nabla^2\chi_0)+k_h\nabla^2\sigma+\hat{Q}, \tag{2.27}$$

$$\frac{\partial q}{\partial t} = -\nabla\cdot(k\times\nabla(\psi-\tau)+\nabla\chi)q)+E-P_c+k_h\nabla^2 q, \tag{2.28}$$

$$b\, c_p\nabla^2\theta = \nabla\cdot(f\nabla\tau), \tag{2.29}$$

and

$$\Delta p\nabla^2\chi_0 = -J(\psi-\tau, P_g), \tag{2.30}$$

$$\psi_0 = \psi-1.6\,\tau \tag{2.31}$$

where

$$b = \tfrac{1}{2}[(\frac{3}{4})^\kappa - (\frac{1}{4})^\kappa] = .124,$$

$$\bar{Q} = \tfrac{1}{2}[(\frac{p_0}{p_3})^\kappa Q_3 + (\frac{p_0}{p_1})^\kappa Q_1]/c_p$$

is the vertically averaged diabatic heating per unit mass, and

$$\hat{Q} = \tfrac{1}{2}[(\frac{p_0}{p_3})^\kappa Q_3 - (\frac{p_0}{p_1})^\kappa Q_1]/c_p$$

is the difference in the diabatic heating per unit mass between the two

layers.

The above system is a set of eight equations with eight unknowns ψ,

τ, θ, σ, χ, χ_0, ψ_0, q. This system will be transformed to the spectral

space using the spherical harmonics as basis functions.

3. Thermal Forcing of the Earth-Atmosphere System

Mechanisms that force the model's atmosphere are either external or internal. The upper layer is heated by short- and longwave radiation, by the lateral diffusion of heat, and by the heat released by a convective adjustment. The lower layer is heated by short- and longwave radiation, lateral diffusion, sensible heat flux from the surface and by latent heat release, and is cooled by the heat transferred upward by the convective adjustment. Evaporation provides a source of water vapor which is also diffused and lost through precipitation.

3.1 Solar radiation

The incoming solar radiation at the top of the model's atmosphere is calculated as a function of daily mean zenith angle (Wetherald and Manabe, 1972). Diurnal variation of the solar energy is excluded. The mean zenith angle $\bar{z}$ is given by

$$\cos \bar{z} = \sin\phi \, \sin\delta + (\cos\phi \, \cos\delta \, \sin H_o)/H_o, \qquad (3.1)$$

where ϕ is the latitude angle, δ is the declination angle, and H_o is the hour angle given by

$$H_o = \cos^{-1} (-\tan\phi \, \tan\delta), \qquad (3.2)$$

$$\delta = 23.45 \sin 2\pi \frac{(N-80)}{360} , \qquad (3.3)$$

N is the number of days measured from day 0 at 00Z at the first of January.

The incoming solar radiation at the top of the atmosphere is given by

$$S_\infty = \bar{S} \, H_o / \pi, \tag{3.4}$$

$$\bar{S} = \quad (\frac{a_m}{a_s})^2 \; S_c \; \cos\bar{z}, \qquad \phi - \delta < \frac{\pi}{2}$$

$$0 \qquad\qquad\qquad \phi - \delta > \frac{\pi}{2}$$

S_c is the solar constant taken to be 1400 w/m². Recent measurements of solar irradiance from earth orbiting satellites (Smith, et al., 1982) give an average value about 1375 w/m². This value is about 1.8% less than the assumed value. Parameters a_s and a_m are the instantaneous and mean distance of the earth from the sun, respectively,

$$\frac{a_s}{a_m} = 1 + .01676 \sin 2\pi \; \frac{(N-94)}{360}. \tag{3.5}$$

The amount of solar radiation absorbed by the earth's atmosphere system is calculated using a formulae given by Kubota (1972). The solar radiation absorbed by the atmosphere S_r is given by

$$S_r = x(1-r_a)S_\infty, \tag{3.6}$$

where x is the absorptivity of the atmosphere taken to be constant = .26. The albedo of the atmosphere, r_a, is calculated taking into consideration the observed mean zonal amount of clouds (Berliand, 1960),

$$r_a = (\alpha + \beta c)c, \tag{3.7}$$

where β is a constant equal to .38, c is the amount of low and medium clouds in tenths of sky cover. Although the model has no explicit modulation of the clouds, they are implicitly included through the atmospheric albedo which affects the solar energy budget. The parameter α is a function of latitude.

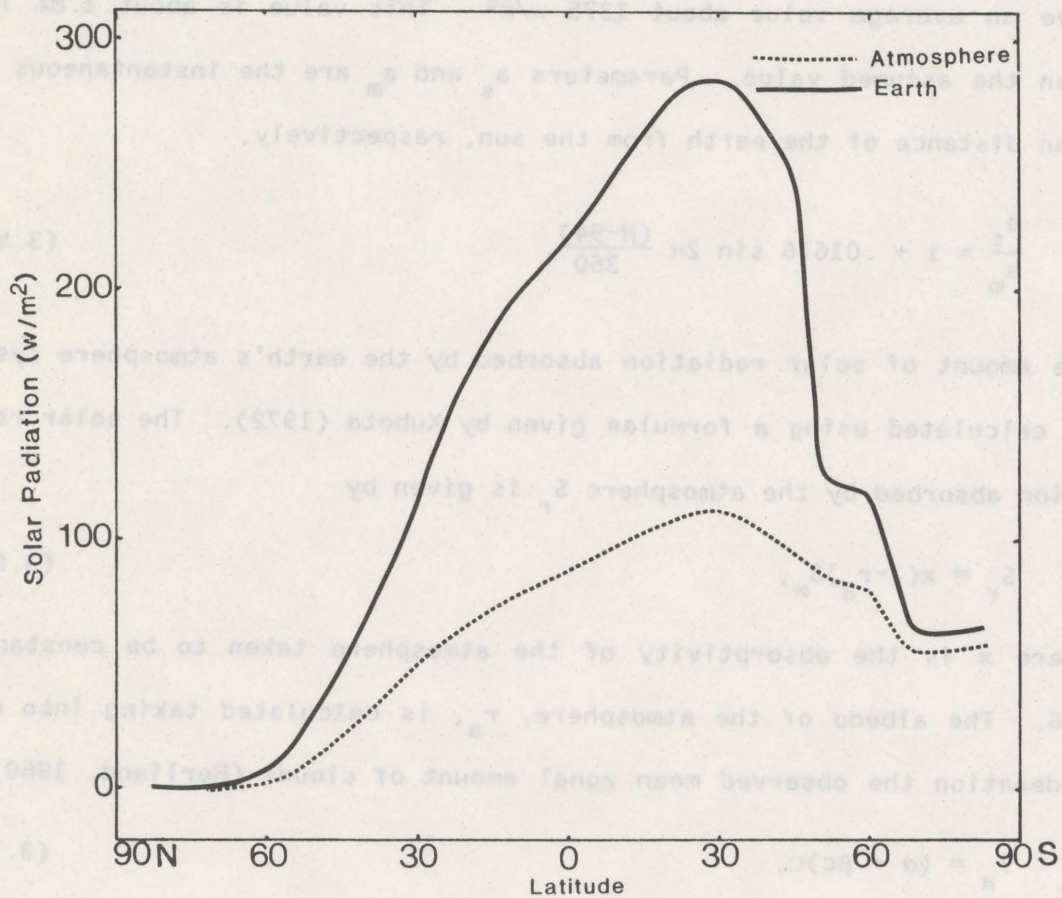Fig. 2. The zonal average of the calculated solar radiation (w/m^2) absorbed by the atmosphere (dotted line) and the earth (full line) for the first of January.

The net solar energy absorbed by the earth's surface is given by

$$S_s = (1-x)(1-r_a)(1-r_s)S_\infty, \tag{3.8}$$

where r_s is the January zonal average albedo of the earth's surface (oceans are not included). The surface albedos are categorized as areas of permanent ice (albedo = .8), partial snow in middle and low latitudes (albedo = .2 to .3), and dense forests (albedo = .15). The values of different parameters used for the January solar radiative calculation are shown in Table 1.

The above formulae give a global average planetary albedo $\cong$ 34%. Stephens et al., (1981), using satellite observations, estimated the global average planetary albedo for January to be 31%. Fig. 2 reveals the calculated solar radiation absorbed by the atmosphere and the earths surface at the first of January.

3.2 Longwave radiation

The calculation of the longwave radiative cooling of the atmosphere makes use of a parameterization of the outgoing infrared radiation (Thompson and Warren, 1982). The parameterization comprises clear sky. Only two parameters are used to predict clear-sky outgoing infrared irradiance: surface air temperature (T_a) and climatological vertical mean relative humidity (RH).

The clear sky outgoing infrared irradiance at the top of the atmosphere is given by

$$L_4 = a_0 + a_1 T_a + a_2 T_a^2 + a_3 T_a^3, \tag{3.9}$$

where

$$a_n = b_{0n} + b_{1n}(RH) + b_{2n}(RH)^2, \quad n = 0, 1, 2, 3. \tag{3.10}$$

The values of the b's are given by,

$$b_{00} = 2.34414 \times 10^2,$$

$$b_{10} = -3.47968 \times 10^1,$$

$$b_{20} = 1.02790 \times 10^1,$$

$$b_{01} = 2.60065 \times 10^0,$$

$$b_{11} = -1.62064 \times 10^0,$$

$$b_{21} = 6.34856 \times 10^{-1},$$

$$b_{02} = 4.40272 \times 10^{-3},$$

$$b_{12} = -2.26092 \times 10^{-2},$$

$$b_{22} = 1.12265 \times 10^{-2},$$

$$b_{03} = -2.05237 \times 10^{-5},$$

$$b_{13} = -9.670 \times 10^{-5},$$

$$b_{23} = 5.62925 \times 10^{-5}.$$

The values of RH used for the January simulation are shown in Table 1. These values are interpolated from the values given by Thompson and Warren (1982).

The model's longwave emissivity is divided between the upper and lower layer by fraction .4 and .6 respectively. The net longwave irradiance at the earth's surface (Deardorff, 1978) is given by

$$L_0 = \varepsilon_g(BT_g{}^4 - yBT_a{}^4) \tag{3.11}$$

where B is the Stephen Boltzman constant, ε_g is the emissivity of the ground surface in the infrared taken to be equal to .95, and y is the parameterization for the effective emissivity of the air which is calculated from the relation

Table 1

Parameters Used for Solar and Longwave Radiation Calculations

Parameter Latitude	Clouds c	Atmospheric Albedo (r_a)	Surface Albedo (r_s)	Average relative humidity (RH)
84.1	0.35	0.096	0.8	.48
76.5	0.41	0.129	0.8	.53
68.9	0.48	0.179	0.8	.58
61.3	0.54	0.305	0.4	.6
53.6	0.56	0.343	0.3	.59
45.9	0.54	0.316	0.2	.58
38.3	0.45	0.248	0.2	.54
30.6	0.37	0.185	0.18	.46
23.	0.28	0.131	0.15	.41
15.3	0.29	0.145	0.14	.38
7.7	0.32	0.167	0.14	.43
0.	0.38	0.207	0.14	.57
-7.7	0.36	0.193	0.12	.53
-15.3	0.35	0.183	0.1	.46
-23.0	0.34	0.166	0.1	.38
-30.6	0.36	0.179	0.1	.35
-38.3	0.42	0.227	0.1	.4
-45.9	0.51	0.293	0.1	.46
-53.6	0.60	0.377	0.5	.50
-61.3	0.62	0.369	0.5	.53
-68.9	0.55	0.8	0.8	.51
-76.5	0.47	0.8	0.8	.46
-84.1	0.40	0.8	0.8	.41

$$y = (c + (1-c)\times.67\times(1670 \ q_a)^{.08}), \tag{3.12}$$

here the value of c, the cloud fraction, is assumed as a global average equal to .5 and q_a is the water vapor mixing ratio near the surface.

3.3 Large scale precipitation and latent heat release

The model has a moisture content in the lower layer (level 1) only. The procedure for large scale precipitation and convective adjustment starts after completing each time step of integration. The mixing ratio at each grid point of the 750 mb level is examined for super-saturation.

If $q(T_1) < \gamma q_s(T_1)$, then no precipitation or convective adjustment takes place. The parameter γ represents a specified critical relative humidity (γ = .85 in this study). T_1 is the temperature at any grid point in level 1, and q and q_s are the mixing ratio and the saturation mixing ratio, respectively.

On the other hand, if $q(T_1) \geq \gamma q_s(T_1)$, condensation occurs with the associated latent heat release. The temperature T_1 will be agumented by an increment ΔT, such that

$$\Delta T = \frac{L}{c_p} (q(T_1) - q_s' (T + \Delta T)), \tag{3.13}$$

where q_s' is the new saturation mixing ratio at the temperature $T+\Delta T$,

$$q_s' = \gamma q_s + \gamma \frac{\partial q_s}{\partial T} \Delta T. \tag{3.14}$$

Using the Clausius-Clapeyron equation, (3.14) takes the form

$$q_s' = \gamma q_s + \gamma \frac{L q_s}{R_v T^2} \Delta T \tag{3.15}$$

where R_v is the water vapor gas constant and L is the latent heat of condensation. The rate of condensation (precipitation) per unit mass, P_c, is given by

$$P_c = (q - q_s')/\Delta t \qquad (3.16)$$

where Δt is the time step of integration. Using (3.13), (3.15) and (3.16)

$$P_c = \frac{q - \gamma q_s}{\Delta t} \left(1 + \frac{\gamma L^2}{c_p R_v T_l^2} q_s\right) \qquad (3.17)$$

It is clear that a relevant form of (3.13) is

$$\Delta T = \frac{L}{c_p} P_c \Delta t. \qquad (3.18)$$

After the release of latent heat in the lower layer as a result of the condensation of water vapor, the atmosphere is tested to see if convective adjustment is required. Convection is assumed to develop if the atmosphere is unstable relative to the moist adiabatic lapse rate Γ_s, then the temperature of the two levels is adjusted to stabilize the model's atmosphere by cooling the lower layer and warming the upper layer, with the vertically averaged temperature conserved. The new lapse rate is the same as Γ_s.

3.4 Net heating of the Earth-Atmosphere system

The way in which the model responds to heating and how it simulates the observed atmospheric heat balance are fundamental aspects of its ability to reproduce the seasonal distributions of global climate. From the previous discussions we can calculate the different partitions of the heating function.

Of basic importance is the net radiation at the top of the atmosphere which represents the net gain or loss of both solar and longwave radiative energy this may be written as

$$N_\infty = S_\infty - r_a S_\infty - r_s (1 - x)(1 - r_a) S_\infty - L_4. \qquad (3.19)$$

On the right side of (3.19) the second and third terms represent the amount of solar radiation reflected by the atmosphere and the earth's surface, respectively, while the last term is the net outgoing longwave radiation at the top of the model atmosphere.

The net radiation at the earth's surface N_s may be written using (3.8) and (3.11) as

$$N_s = (1-x)(1-r_a)(1-r_s)S_\infty - L_0. \tag{3.20}$$

The net surface heating, B_s, is given by

$$B_s = N_s - Q_s - LE, \tag{3.21}$$

It is assumed that $B_s=0$, and the resulting equation is used to determine the surface ground temperature T_g. Over the water surfaces, on the other hand, the surface temperature is assigned and B_s is not required to be zero.

The net atmospheric heating may be considered by combining the net radiation at the top of the atmosphere (3.19), the net surface heat flux (3.21), and the internal release of latent heat accompanying condensation (here precipitation). Recognizing that the surface evaporation removes heat from the water source and therefore it is not a part of the atmospheric heating, we may write the net heating of the atmosphere, B_a, as

$$B_a = x(1-r_a)S_\infty + L_0 - L_4 + Q_s + LP_c. \tag{3.22}$$

This expression for B_a is also equal to the sum of the atmospheric storage of total energy and the divergence of the atmospheric total energy flux.

Finally, we may combine the net surface heating (3.21) and the net atmospheric heating (3.22) in order to get the net heating of the

combined earth-atmosphere system. This heating is given by

$$B_{ea} = N_\infty + L(P_c - E) \qquad (3.23)$$

This may be regarded as the balance of total energy in the earth-atmosphere system.

3.5 Surface temperature

The surface temperature, T_g, is used to calculate the bulk formulae (2.15) and (2.17). As mentioned before the surface temperatures of the water are specified as the climatological values of January. On land and ice surfaces the temperature is calculated from the surface thermal energy balance (3.21) assuming negligible heat capacity of the earth ($B_s = 0$) (Holloway and Manabe, 1971). Over oceanic locations assumed to be covered with ice, $B_s = 0$ is also assumed, but with a term representing the heat conduction through the ice (depending on the difference between the ice surface temperature and the freezing point of water) added to the right hand side of (3.21). Over all ice and snow covered surfaces the computed surface temperature is not permitted to rise above 0°C. In such a case the excess heat is assumed to be used in melting. Equation (3.21) can take the form

$$B_s = N_s - Q_s - LE + I(T_g - 271.2). \qquad (3.24)$$

The last term on the right hand side represent the effect of heat conduction from unfrozen water below sea ice in the polar latitudes of the Northern Hemisphere. Assuming the thermal conductivity of ice, $T_c = 2.1$ J m^{-1} °K^{-1} sec^{-1}, the temperature of the underlying water is 271.2°K and the ice layer thickness d = 2 m, then the constant $I = T_c/d = 1.05$ w/m² °K^{-1}. This term is needed to prevent unrealistically cold temperatures in the Northern Hemisphere polar regions during winter.

Appendix I explains the method of solving (3.24). The Newton iteration method is used and is found to be efficient in solving such type of equations.

4. Numerical Simulation

The conventional spectral method is Galerkin's method based on ex-
panding the different variables with a truncated series of surface
spherical harmonics. The method is used for the numerical integration
of the hydrodynamical equations. Two types of expansion are often used,
the triangular and rhomboidal truncations. The advantages of the spec-
tral method over the usual finite difference methods are summarized as
follows (Machenhauer, 1974):

1) The nonlinear terms are alias free, which prohibits the exis-
   tence of the nonlinear instability described by Phillips (1959).

2) Quadratic area integral invariants like the kinetic energy and
   enthalpy also are invariant for the truncated system, since the
   error fields are orthogonal to the variables.

3) Linear terms are computed without any truncation error.

4) No special treatment is required for dealing with the polar
   region when using the vorticity and divergence fields. By con-
   trast, in the finite difference method the horizontal wind com-
   ponents are discontinuous at the pole.

5) The friction term of the finite difference methods is necessary
   to prevent aliasing instability. It also is necessary for the
   removal of energy from the shortwave end of the spectrum. When
   using the spectral method, it also is important to prevent blocking
   of energy at the highest wave numbers retained, but in this case
   the purpose is only a simulation of the effect of the small scales
   not retained in the representation.

A study by Hoskins and Simmons (1974) compared finite difference and spectral models. The study showed that no one method has a superiority in all respects. In comparison with the finite difference model, the spectral model gave much improved solutions for the amplitudes and phases of the predicted waves. On the other hand, the finite difference model gave a more accurate representation of the frontal systems.

It is of interest to compare the two types of truncation mentioned before, namely the rhomboidal and triangular. For the same zonal wave number truncation, the triangular representation has fewer degrees of freedom than the rhomboidal and hence requires less computing time. If we retain the same degrees of freedom in both the triangular and rhomboidal truncations, the former will be more appropriate for mean zonal fields than the latter. At the same time the rhomboidal truncation could introduce higher wave numbers, namely the eddies. The same study by Hoskins and Simmons (1974) did not give a definite conclusion concerning the comparison between rhomboidal and triangular truncation. In some experiments the rhomboidal truncation gave a more accurate approximation to the solution than the triangular truncation. In other experiments the triangular truncation gave a more efficient description of Rossby wave instability.

In this study we used the rhomboidal truncation since it gives a comparable resolution in both horizontal directions.

4.1 Spectral method

The dependent variables ψ, τ, χ, χ_o, θ, σ, q are expanded in truncated series of the form

$$X(\mu,\lambda) = \sum_{m=-M}^{M} \sum_{n=|m|}^{|m|+J} X_n^m \, Y_n^m(\mu,\lambda) \qquad (4.1)$$

where X is any variable being studied, X_n^m are harmonic coefficients, λ is longitude, μ is the sine of latitude, m is the zonal wavenumber, n is the degree of a spherical harmonic component, $n-|m|$ is a meridional wavenumber in the sense that there are $n-|m|$ zero crossings of Y_n^m between equator and pole, M is the highest zonal wave number retained in the truncated series, and J is the highest value of $n-|m|$ retained in the truncated series. Y_n^m are spherical harmonic functions defined by

$$Y_n^m = P_n^m (\mu) \, e^{im\lambda}. \tag{4.2}$$

P_n^m are the Associated Legendre functions of the first kind

$$P_n^m(\mu) = (\frac{(2n+1)}{4\pi} \frac{(n-m)!}{(n+m)!})^{\frac{1}{2}} \frac{(1-\mu^2)^{|m|/2}}{2^n n!} \frac{d^{n+|m|}}{d\mu^{n+|m|}} (\mu^2-1)^n \tag{4.3}$$

A spherical harmonic coefficient is defined by

$$X_n^m = \frac{1}{4\pi} \int_0^{2\pi} \int_{-1}^{+1} X \, Y_n^{m*} \, d\mu d\lambda \tag{4.4}$$

where Y_n^{m*} is the complex conjugate of Y_n^m.

Y_n^m are orthogonal over the surface of the sphere, i.e.

$$\frac{1}{4\pi} \int_0^{2\pi} \int_{-1}^{+1} Y_n^m Y_{n_1}^{m_1*} \, d\mu d\lambda = \begin{cases} 1 \text{ for } (m_1,n_1) = (m,n) \\ 0 \text{ for } (m_1,n_1) \neq (m,n) \end{cases}, \tag{4.5}$$

and are eigenfunctions of the Laplacian operator

$$\nabla^2 Y_n^m = -n \frac{(n+1)}{a^2} Y_n^m, \tag{4.6}$$

where a is the radius of the sphere. The coefficients for negative and positive values of m are related in the following way:

$$X_n^{-m} = (-1)^m X_n^{m*}.$$

Nonlinear terms are transformed from grid point space to spectral space using the full transform method (Machenhauer and Rasmussen, 1972; Orszag, 1970). The method is computationally highly efficient relative to the interaction coefficient method for $J \geq 9$.

The procedure for calculating the spectral coefficients of the nonlinear terms using the full transform method is as follows:

1) Calculate the nonlinear terms at each grid point in physical space.

2) Transform to the Fourier space at each Gaussian latitude, using fast Fourier transform routines.

3) Transform to the spectral space using the Gaussian quadrature formula.

Highly nonlinear terms, like diabatic heating terms cause problems in finding their spectral transforms. This problem is resolved by using the full transform method. They are calculated in physical space, then added to the nonlinear dynamic terms, and the whole sum is transformed to spectral space.

To guarantee an alias-free solution, there are two conditions that must be fulfilled (Machenhauer and Rasmussen, 1972). These conditions specify the minimum number of zonal grid points, N_g, and the minimum number of Gaussian latitudes, I_s, on the sphere:

$N_g > 3 M + 1$

$I_s > M + 3/2 J$.

In case of the rhomboidal truncation (M = J) used here, the latter condition is

$I_s > 5/2 M$.

For the simulation with wavenumber 9, $N_g = 32$ and $I_s = 23$. On the other hand, for wave number 15 simulation, $N_g = 48$ and $I_s = 40$.

To transform the system (2.24 - 2.31) to its spectral form, each variable is expanded using (4.1). The resulting equations are multiplied by Y_n^{m*} and integration of both sides is performed using equations (4.4 - 4.6). The nonlinear terms are calculated using the transform method mentioned before.

The system of equations in its spectral form is given by

$$\dot{\psi}_n^m = -\frac{a^2}{n(n+1)} \{-J(\psi,\nabla^2\psi) - J(\tau,\nabla^2\tau)\}_n^m + \frac{2\Omega m}{n(n+1)} i\, \psi_n^m -$$

$$\Omega \left(\frac{n+2}{n+1} D_{n+1}^m (\chi_0)_{n+1}^m + \frac{n-1}{n} D_n^m (\chi_0)_{n-1}^m\right) \qquad (4.7)$$

$$-\frac{k_s}{2}(\psi_0)_n^m - K_h\, n\, \frac{(n+1)}{a^2}\, \psi_n^m + \frac{2k_h}{a^2}\, \psi_n^m ,$$

$$\dot{\tau}_n^m = \frac{-a^2}{n(n+1)} \{(-J(\tau,\nabla^2\psi) - J(\psi,\nabla^2\tau))\}_n^m + \frac{2\Omega m}{n(n+1)} i\, \tau_n^m -$$

$$\Omega \left(\frac{n+2}{n+1} D_{n+1}^m (\chi_0)_{n+1}^m + \frac{n-1}{n} D_n^m (\chi_0)_{n-1}^m\right)$$

$$+ \frac{k_s}{2}(\psi_0)_n^m - 2k_d\, \tau_n^m - k_h\, n\, \frac{(n+1)}{a^2}\, \tau_n^m + \frac{2k_h}{a^2}\, \tau_n^m \qquad (4.8)$$

$$+ 2\Omega \left(\frac{n+2}{n+1} D_{n+1}^m \chi_{n+1}^m + \frac{(n-1)}{n} D_n^m \chi_{n-1}^m\right),$$

$$\dot{\theta}_n^m = \{-J(\psi,\theta) - J(\tau,\sigma) - \tfrac{1}{2}(\nabla\chi_0 \cdot \nabla\theta + \nabla\chi_0 \cdot \nabla\sigma + 3\sigma\nabla^2\chi_0)\}_n^m$$

$$\qquad (4.9)$$

$$- n\, \frac{(n+1)}{a^2}\, k_h\, \theta_n^m + (\nabla \cdot (\sigma\nabla\chi))_n^m + \bar{Q}_n^m ,$$

$$\dot{\sigma}_n^m = \{- J(\psi,\sigma) - J(\tau,\theta) - \tfrac{1}{2}(\nabla\chi_0 \cdot \nabla\theta + \nabla\chi_0 \cdot \nabla\sigma - \sigma\nabla^2\chi_0)\}_n^m$$

$$+ (\nabla\chi \cdot \nabla\theta)_n^m - n\frac{(n+1)}{a^2} k_h \sigma_n^m + \hat{Q}_n^m , \qquad (4.10)$$

$$\dot{q}_n^m = - (\nabla \cdot ((k\times\nabla(\psi-\tau) + \nabla\chi)q))_n^m - n\frac{(n+1)}{a^2} k_h q_n^m + (E-P_c)_n^m , \qquad (4.11)$$

$$b \, c_p \, \theta_n^m = 2\Omega(\frac{n+2}{n+1} D_{n+1}^m \tau_{n+1}^m + \frac{(n-1)}{n} D_n^m \tau_{n-1}^m), \qquad (4.12)$$

$$(\Psi_0)_n^m = \psi_n^m - 1.6 \, \tau_n^m, \qquad (4.13)$$

and

$$(\chi_0)_n^m = \frac{2a^2}{n(n+1)} \{J(\psi-\tau), \frac{P_g}{P_o}\}_n^m, \qquad (4.14)$$

where $i = \sqrt{-1}$. The spectral transform of terms of the form $\nabla \cdot (f\nabla\tau)$ or $\nabla \cdot (f\nabla\chi)$ is shown in Appendix (II).

It must be noted that by solving (4.8), (4.9) and (4.12) we can obtain an equation for χ. The equations are simplified and solved as a system of tridiagonal matrices (Appendix III) to find the spectral coefficients of χ that satisfy the linear balance approximation. The simplification is needed to treat the term $(\nabla \cdot \sigma\nabla\chi)$ in (4.9). To do this, we split σ into its global average $[\sigma]$, and the deviation from this average σ',

$$\sigma = [\sigma] + \sigma'.$$

Then

$$\nabla \cdot (\sigma\nabla\chi) = [\sigma]\nabla^2\chi + \nabla \cdot (\sigma'\nabla\chi).$$

The first term on the right side of the above equation is of a larger

order of magnitude and is added to the other unknown terms, which in-

clude χ. The smaller, second term, is considered as a known parameter

and calculated using the values of χ at the previous time step. The

method is found to be stable. It significantly reduces the number of

calculations at this stage.

4.2 Energetics of the model

The two layer model discussed here conserves the sum of kinetic and

available potential energy under reversible adiabatic processes (Lorenz,

1960). If one introduces the topographical forcing as a lower boundary

vertical velocity, it is hard to verify the energy conservation (Burger

and Riphagen, 1979). It is only the very simple lower boundary condi-

tion $\omega_0 = 0$ (used by Lorenz) at $p = 1000$ mb that guarantees an energy-

conserving system.

The kinetic and available potential energies, KE and AP, respec-

tively, are expressed in the forms

$$KE = \frac{\Delta p}{g}(\nabla\psi \cdot \nabla\psi + \nabla\tau \cdot \nabla\tau) \tag{4.15}$$

and

$$AP = \frac{2b}{g} \frac{c_p \Delta p}{g} \frac{[(\theta')^2 + (\sigma')^2]}{[\sigma] + [\sigma^2 + (\theta')^2 + (\sigma')^2]^{\frac{1}{2}}} . \tag{4.16}$$

The square brackets [ ] indicate the global area average and the dashes

indicate the deviation from that average.

In spectral space the kinetic and available potential energy within

a spherical harmonic mode are given by

$$(KE)_n^m = \frac{\Delta p}{ga^2} ((\psi_n^m)^2 + (\tau_n^m)^2) \, n(n+1) \, (2-\delta_{0m}), \text{ for } m \geq 0 \tag{4.17}$$

and

$$(AP)^m_n = \frac{2b\, c_p\, \Delta p}{g} \frac{((\theta^m_n)^2 + (\sigma^m_n)^2)\,(2-\delta_{0m})}{\sigma^0_0 + \{\underset{rs}{\Sigma\Sigma}(\theta^r_s)^2 + (\sigma^r_s)^2 - (\theta^0_0)^2\}^{\frac{1}{2}}},$$ (4.18)

for $n \neq 0$ $m \geq 0$, where $\delta_{00} = 1$ and $\delta_{0m} = 0$ for $m > 0$.

4.3 Initial conditions and time integrations

The model integration starts from a hypothetical, horizontally isothermal, atmosphere at rest with a moist adiabatic lapse rate. The model runs for 120 days assuming perpetual solar forcing (first of January). This initialization procedure is used in order to reach a statistically steady state. After that the solar declination is changed daily to simulate the climates of January (days 121-150), February (days 151-180), and March (days 181-210). These runs are considered as control runs for the comparable periods within the experiments.

The time difference method used is the centered (leap-frog) scheme. To avoid the growth of unnecessary computational modes, a time smoother was used on the prognostic variables (Asselin, 1972) at every time step. The diffusion are calculated using values at the previous time step to ensure computational stability. The time step used is 2 hours. Appendix IV shows a flow diagram of the calculation procedure.

5. Summary

In this report a two-level global spectral model is developed. In spite of the dynamical and physical simplifications, the model could be used to simulate the atmospheric large scale circulation. The model is suitable for climate sensitivity experiments in middle and high latitudes of both hemispheres. The efficient computer runs of the model (30 day integration, for wave number 9 truncation, requires about 50 sec of CPU time using CRAY-1 machine) enable us to perform many experiments and test several hypotheses before using the complicated multilevel primitive equation models.

The two levels representing the model's atmosphere are 750 mb and 250 mb. The surface is assumed at 1000 mb. The model retains the nonlinear interactions between dependent variables. Nonlinear interactions are important components of midlatitude synoptic motions. Additionally, for climate sensitivity studies nonlinear interactions are potentially significant since linear solutions are resonant or nearly resonant while nonlinear solutions are not. The present model uses a moisture budget equation at the 750 mb level with moist convective adjustment between the two layers. The advection by the divergent wind is retained. Temperature and heat fluxes in each layer can differ through a variable static stability.

The physical forcing is parameterized with reasonable simplicity to include the major forcing mechanisms which develop the large scale atmospheric circulation. The solar energy is specified as a function of latitude and time assuming a daily mean zenith angle. Longwave radiation forcing of the two layers and the surface are calculated. The mechanical effects of orography are introduced in the form of a lower

boundary vertical velocity. The differential diabatic heating due to the distribution of land and sea also is included. The sea surface temperatures are specified using the observed January mean values. On continents and ice surfaces the thermal energy balance equation is solved for the surface temperature. Both orography and differential heating between land and sea are importnat for producing a correct phase and amplitude of the middle latitudes ultralong waves in linear atmospheric models.

A relatively straightforward extension, not yet attempted, is the parameterization of upper level clouds and their associated radiative effects. Such future work is envisaged for studying the role of high clouds for short-term climate and the earth's radiation budget.

References

Asselin, R., 1972: Frequency filter for time integrations. Mon. Wea. Rev., 100, 487-490.

Berkufsky, L. and E.A. Bertoni, 1955: Mean topographic charts for the entire earth. Bull. Amer. Met. Soc., 36, 350-354.

Berliand, T.G., 1960: Methods for climatological computation of global radiation. Meteorol. Hydrol., No. 6.

Bolton, D., 1980: The computation of equivalent potential temperature. Mon. Wea. Rev., 108, 1046-1053.

Budyko, M.I., 1969: The effect of solar radiation variations on the climate of the earth. Tellus, 21, 611-619.

Burger, A.P., and H.A. Riphagen, 1979: The lower boundary condition and energy consistency in primitive and filtered models. J. Atmos. Sci., 36, 1436-1449.

Charney, J.G., 1959: On the theory of the general circulation of the atmosphere. The atmosphere and the sea in motion. New York, The Rockefeller Institute Press, 135-162.

Chervin, R.M., J.E. Kutzbach, D.D. Houghton, and R.G. Gallimore, 1980: Response of the NCAR general circulation model to prescribed changes in ocean surface temperature. Part II: Midlatitude and subtropical changes. J. Atmos. Sci., 37, 308-404.

Corby, G.A., A. Gilchrist, and P.R. Rowntree, 1977: United Kingdom Meteorological Office five-level general circulation model. Methods in Compt. Phys., 17, 67-110.

Deardorff, J.W., 1978: Efficient prediction of ground surface temperature and moisture, with inclusion of a layer of vegetation. J. Geophys. Res., 83, 1889-1903.

Haltiner, G.J., 1971: Numerical Weather Prediction. John Wiley & Sons, Inc., 317 pp.

Haltiner, G.J., and R.T. Williams, 1980: Numerical Prediction and Dynamic Meteorology. John Wiley & Sons, Inc., 477 pp.

Held, I.M., and M. Suarez, 1978: A two level primitive equation atmospheric model designed for climate sensitivity experiments. J. Atmos. Sci., 35, 206-228.

Holloway, J.L., and S. Manabe, 1971: Simulation of climate by a global general circulation model. Mon. Wea. Rev., 99, 335-370.

Hoskins, B.J., and A.J. Simmons, 1974: The development of spectral models in the U.K. Universities atmospheric modelling group. The GARP programme on numerical experimentation. Report No. 7, 94-99.

Kasahara, A., and W.M. Washington, 1971: General circulation experiments with a six-layer NCAR model, including orography cloudiness and surface temperature calculations. J. Atmos. Sci., 28, 657-701.

Kikuchi, Y., 1969: Numerical simulation of the blocking process. J. Met. Soc. Japan, 47, 29-54.

Kubota, I., 1972: Calculation of seasonal variation in the lower tropospheric temperature with heat budget equations. J. Met. Soc. of Japan, 50, 18-35.

Lorenz, E., 1960: Energy and numerical weather prediction. Tellus, 12, 364-373.

Lorenz, E., 1961: Simplified dynamic equations applied to the rotating-basin experiments. J. Atmos. Sci., 19, 39-51.

Machenhauer, B., 1974: On the present state of spectral methods in numerical integrations of global atmospheric models. The GARP programming on numerical experimentation., Report No. 7, 1-21.

Machenhauer, B., and E. Rasmussen, 1972: On the integration of the spectral hydrodynamical equations by a transform method. Univ. of Copenhagen, Rpt. No. 3, 44 pp.

Manabe, S., J. Smagorinsky, and R.F. Strickler, 1965: Simulated climatology of a general circulation model with a hydrologic cycle. Mon. Wea. Rev., 93, 769-798.

Orszag, S.A., 1970: Transform method for the calculation of vector-coupled sums: Application to the spectral form of the vorticity equation. J. Atmos. Sci., 27, 890-895.

Otto-Bliesner, B.L., G.W. Branstator, and D.D. Houghton, 1982: A global low-order spectral general circulation model. Part I: formulation and seasonal climatology. J. Atmos. Sci., 39, 929-948.

Phillips, N.A., 1959: An example of nonlinear computational instability. The atmosphere and the sea in motion. New York, The Rockefeller Institute Press, 501-504.

Puri, K., and W. Bourke, 1974: Implications of horizontal resolution in spectral model integrations. Mon. Wea. Rev., 102, 333-347.

Roads, J.O., and R.C.J. Somerville, 1982: Predictability of ultralong waves in global and hemispheric quasi-geostrophic barotropic models. J. Atmos. Sci., 39, 745-755.

Salmon, R., and M.C. Hendershott, 1976: Large scale air-sea interactions with a simple general circulation model. Tellus, 18, 228-242.

Sellers, W.D., 1973: A new global climate model. J. Appl. Met., 12, 241-254.

Smith, E.A., T.H. Vonder Haar, and J.R. Hickey, 1983: The nature of the short period fluctuations in solar irradiance received by the earth. Climatic Change, 5, 211-235.

Stephens, G.L., G.G. Campbell, and T.H. Vonder Haar, 1981: Earth
radiation budgets. J. of Geophys. Res., 86, 9739-9760.

Thompson, S.L. and S.G. Warren, 1982: Parameterization of outgoing
infrared radiation derived from detailed radiative calculations.
J. Atmos. Sci., 39, 2667-2680.

Wetherald, R.T., and S. Manabe, 1972: Response of the joint ocean-
atmospheric model to the seasonal variation of the solar radiation.
Mon. Wea. Rev., 100, 42-59.

Wielicki, B. and M. Hendershott, 1979: Further development of a spec-
trally truncated model atmosphere for climate studies. Dyn. Atmos.
and Oceans, 3, 453-464.

APPENDIX I

The Solution of the Surface Thermal

Energy Balance Equation

Using equations (3.8), (3.11), (3.20), (3.21) and (3.24), the steady-state surface thermal energy balance is represented by

$$B_s = S_s - \varepsilon_g BT_g^4 + \varepsilon_g yBT_a^4 - Q_s - LE + I(T_g - 271.2),$$

where

$$Q_s = \rho_s c_p c_d |v_0|(T_g - T_a),$$

and $LE = L \rho_s c_d |v_0| GW(q_s(T_g) - h q_s(T_a)).$

We define I_1 and I_2 such that

$$I_1 = \rho_s c_p c_d |v_0|$$

and

$$I_2 = L \rho_s c_d |v_0|$$

The above equation can be written in the form

$$F(T_g) = S_s - \varepsilon_g BT_g^4 + \varepsilon_g yBT_a^4 - I_1(T_g - T_a) - I_2(q_s(T_g)$$
$$- hq_s(T_a)) - I(T_g - 271.2). \qquad (A1.1)$$

(A1.1) is solved for T_g, using Newtons iteration method.

Differentiating (A1.1) with respect to T_g we obtain

$$F'(T_g) = -4\varepsilon_g BT_g^3 - I_1 - I_2 q_s'(T_g) - I. \qquad (A1.2)$$

To calculate the saturation mixing ratio, $q_s(T_g)$, and its derivative, $q'(T_g)$, we use a formula for the saturation vapor pressure, e_s (Bolton, 1979). This formula provides an accuracy of 0.1% in the range $-30°C < T_g < 35°C$.

$$e_s(T_g) = 6.112 \exp (17.67 (T_g - 273.15)/(T_g - 29.65)) \qquad (A1.3)$$

$$q_s(T_g) = \frac{.622 \ e_s(T_g)}{p - e_s(T_g)} \qquad \qquad \text{(A1.4)}$$

Differentiating (A1.4) with respect to T_g,

$$q_s'(T_g) = \frac{q_s p e_s'(T_g)}{(P - e_s)} \qquad \qquad \text{(A1.5)}$$

and using (A1.3), one obtains

$$e_s'(T_g) = \frac{17.67 \times 243.15}{(T_g - 29.65)^2} \quad . \qquad \qquad \text{(A1.6)}$$

Substituting (A1.5) into (A1.2), we arrive at

$$F'(T_g) = - 4\varepsilon_g B T_g^3 - I_1 - I_2 \frac{q_s P \times 4302.645}{(p - e_s(T_g))(T_g - 29.65)^2} - I. \qquad \text{(A1.7)}$$

Using (A1.1) and (A1.7), the solution is convergent in the form

$$T_g^{v+1} = T_g^v - \frac{F(T_g^v)}{F'(T_g^v)}, \qquad \qquad \text{(A1.8)}$$

where the superscripts v and $v+1$ indicate successive iteration steps. Iteration is performed until $F(T_g)$ is less than a small, predetermined value.

APPENDIX II

Spectral Transform of $(\nabla \cdot f \nabla \chi)$

The term $(\nabla \cdot f \nabla \chi)$ can be expanded in the form

$$\nabla \cdot f \nabla \chi = \nabla f \cdot \nabla \chi + f \nabla^2 \chi.$$

Since $f = 2\Omega\mu$,

$$\nabla \cdot f \nabla \chi = \frac{2\Omega}{a^2} (1-\mu^2) \frac{\partial \chi}{\partial \mu} + 2\Omega\mu\nabla^2\chi. \qquad (A2.1)$$

If we expand χ in terms of spherical harmonics defined by (4.1), then

$$\nabla \cdot f \nabla \chi = \frac{2\Omega}{a^2} \sum_{mn} \chi_n^m (1-\mu^2) \frac{\partial Y_n^m}{\partial \mu} - \frac{2\Omega}{a^2} \sum_{mn} n(n+1) \chi_n^m \mu Y_n^m, \qquad (A2.2)$$

or

$$\nabla \cdot (f \nabla \chi) = \frac{2\Omega}{a^2} \sum_{mn} \chi_n^m \{-(n^2-1)D_n^m Y_{n-1}^m - n(n+2) D_{n+1}^m Y_{n+1}^m\}, \qquad (A2.3)$$

where we have used the two recurrence relations

$$(1 - \mu^2) \frac{\partial Y_n^m}{\partial \mu} = (n+1) D_n^m Y_{n-1}^m - n D_{n+1}^m Y_{n+1}^m, \qquad (A2.4)$$

and

$$\mu Y_n^m = D_{n+1}^m Y_{n+1}^m + D_n^m Y_{n-1}^m, \qquad (A2.5)$$

with

$$D_n^m = \left(\frac{n^2-m^2}{4n^2-1}\right)^{\frac{1}{2}}$$

Applying the transform operator (4.4) on (A2.3) and using (4.5), we obtain

$$(\nabla \cdot f \nabla \chi)_n^m = \frac{-2\Omega}{a^2} (n(n+2) D_{n+1}^m \chi_{n+1}^m + (n^2-1) D_n^m \chi_{n-1}^m). \qquad (A2.6)$$

APPENDIX III

Calculation of the Velocity Potential

To establish the linear balance approximation, equations (4.8), (4.9) and (4.12) need to be solved in order to calculate the array χ that satisfy the linear balance relation. This appendix describes the calculation procedure to find χ.

Using the recurrence formula described in Appendix II, equation (4.8) can be written in the form

$$(\dot{\tau})_n^m = -\frac{a^2}{n(n+1)}(R_\tau)_n^m + 2\Omega\left(\frac{n+2}{n+1}D_{n+1}^m\chi_{n+1}^m + \frac{n-1}{n}D_n^m\chi_{n-1}^m\right), \quad (A3.1)$$

where $(R_\tau)_n^m$ is the spherical harmonics of the linear and nonlinear terms that does not contain χ.

Similarily, equation (4.9) can be written in the form

$$(\dot{\theta})_n^m = (R_\theta)_n^m + (\nabla\cdot(\sigma\nabla\chi))_n^m, \quad (A3.2)$$

where $(R_\theta)_n^m$ is the same as the definition of $(R_\tau)_n^m$ but for the thermodynamic equation.

The generalized thermal wind equation (4.12) can be differentiated with respect to time to give the form

$$(\dot{\theta})_n^m = \frac{2\Omega}{bc_p}\left(\frac{n+2}{n+1}D_{n+1}^m\dot{\tau}_{n+1}^m + \frac{n-1}{n}D_n^m\dot{\tau}_{n-1}^m\right). \quad (A3.3)$$

substituting the appropriate indices of (A3.1) and (A3.2) into (A3.3), we can get the diagnostic equation for χ in the form,

$$A(n,m)\chi_{n+2}^m + B(n,m)\chi_n^m + C(n,m)\chi_{n-2}^m + E(n,m)(R_\tau)_{n+1}^m$$

$$+ G(n,m)(R_\tau)_{n-1}^m = (\nabla\cdot(\sigma\nabla\chi))_n^m + (R_\theta)_n^m, \quad (A3.4)$$

where

$$A(n,m) = \frac{4\Omega^2}{bc_p} \frac{n+3}{n+1} D^m_{n+1} D^m_{n+2},$$

$$B(n,m) = \frac{4\Omega^2}{bc_p} \left(\frac{n(n+2)}{(n+1)^2} (D^m_{n+1})^2 + \frac{(n-1)(n+1)}{n^2} (D^m_n)^2 \right),$$

$$C(n,m) = \frac{4\Omega^2}{bc_p} \frac{n-2}{n} D^m_n D^m_{n-1},$$

$$E(n,m) = \frac{2\Omega}{bc_p} \frac{n+2}{n+1} D^m_{n+1},$$

$$G(n,m) = \frac{2\Omega}{bc_p} \frac{n-1}{n} D^m_n.$$

The system (A3.4) needs the transformation of $(\nabla \cdot \sigma \nabla \chi)$ in order to be solved. In such case the gaussian elimination method can be used to solve for χ. However, by making the approximation described in the text the system ends to a tridiagonal matrix which is more efficient to solve than using the gaussian elimination method.

APPENDIX IV

Program Description

Calculations for this model are contained in three programs. Two of them produce input to the model: orography harmonics, ocean temperatures, legendre polynomial coefficients, gaussian latitudes, gaussian coefficients. The results of those two programs are stored on the files:

	orography harmonics	legendre polynomials, etc.
Wave number 9	ADELH1	ADELH4
Wave number 15	ADELH2	ADELH3

The third program calculates the time evolution of the general circulation. The results of the first 120 days of integration with fixed solar radiation for wave number 9 with topography, are stored on file ADRES2. The same but without topography is on file ADRES3. Subroutines for this program are compiled and stored on file ADELH9 for wave number 9 and on ADEL15 for wave number 15.

Table A1. Schematic representation of the sequence of operations

	Subprograms
Reading input data: gaussian coefficients, sin of gaussian latitudes, legendre polynomials and their derivative, ocean temperatures, spectral coefficients of topography and results from previous runs (spectral coefficients)	→ RDTAPE
Initial conditions for statistical calculations	
Daily solar forcing - solar radiation absorbed by the earth, solar radiation absorbed by atmosphere	← → SOLA
Mountain effect - vertical velocity of the lower boundary (surface velocity potential) (in spectral space)	→ OROG ADTO
Humidity flux (phys. space) - transformation to spectral space	→ TR1
Transformation to Fourier space	→ RM1,RM2
Transformation to grid points (using FFT)	→ FFT991
Diabatic heating terms at gaussian latitudes	→ SURFT,EFAP,SNLT,FLON
Nonlinear terms at gaussian latitudes	
Transformation to the Fourier, then to spherical harmonic space	→ FFT991,GUASS
Adding linear contributions for tendencies (RHS of prognostic equations but without terms containing velocity potential)	
Solve for velocity potential to satisfy linear balance	→ SITER,ADTO
Centered time integration with smoothing	→ TIME
Transformation of the vapor mixing ratio and temperature to grid point domain	→ TR2
Convective adjustment	→ CONVEC
Transformation of the mixing ratio and temperatures to the spectral space	→ TR1
Calculation of τ from linear balance equation, with τ(1,M) calculated in subroutine TIME as a boundary condition	→ BAL
Statistical calculation - monthly, zonal averaging	→ ZAV
Writing results	

Time loop

Table A2: The most important variables in the program.

Physical Space:

$$F_1 = -(1-\mu^2)\frac{\partial\psi}{\partial\mu}$$

$$F_{15} = \theta$$

$$F_2 = \frac{\partial}{\partial\lambda}(\nabla^2\psi)$$

$$F_{17} = (1-\mu^2)\frac{\partial}{\partial\mu}(qv)$$

$$F_3 = \frac{\partial\psi}{\partial\lambda}$$

$$F_{18} = \frac{\partial}{\partial\lambda}(qu)$$

$$F_4 = -(1-\mu^2)\frac{\partial}{\partial\mu}\nabla^2\psi$$

$$F_{19} = \sigma$$

$$F_5 = -(1-\mu^2)\frac{\partial\tau}{\partial\mu}$$

$$F_{20} = \nabla^2\chi$$

$$F_6 = \frac{\partial}{\partial\lambda}(\nabla^2\tau)$$

$$F_{21} = q$$

$$F_7 = \frac{\partial\tau}{\partial\lambda}$$

$$F_{22} = -(1-\mu^2)\frac{\partial\eta}{\partial\mu}$$

$$F_8 = -(1-\mu^2)\frac{\partial}{\partial\mu}(\nabla^2\tau)$$

$$F_{23} = \frac{\partial\eta}{\partial\lambda}$$

$$F_9 = -(1-\mu^2)\frac{\partial\theta}{\partial\mu}$$

$$F_{24} = \nabla^2\chi_0$$

$$F_{10} = \frac{\partial\theta}{\partial\lambda}$$

$$F_{25} = -(1-\mu^2)\frac{\partial\chi_0}{\partial\mu}$$

$$F_{11} = -(1-\mu^2)\frac{\partial\sigma}{\partial\mu}$$

$$F_{26} = \frac{\partial\chi_0}{\partial\lambda}$$

$$F_{12} = \frac{\partial\sigma}{\partial\lambda}$$

$$F_{13} = -(1-\mu^2)\frac{\partial\chi}{\partial\mu}$$

$$F_{14} = \frac{\partial\chi}{\partial\lambda}$$

where: ψ = stream function
τ = shear
θ = potential temperature
σ = static stability
χ = velocity potential
q = mixing ratio
$\eta = p_g/\Delta P$ = normalized surface pressure
χ_0 = surface velocity potential
μ = $\sin\ell$ (ℓ = latitude)
λ = longitude

Table A3: The most important variables in the program.

Spectral Space:

$X = \psi$ = stream function

$TO = \tau$ = shear

$PT = \theta$ = mean potential temperature

$SI = \sigma$ = static stability

$Q = q$ = wake vapor mixing ratio

$RK = \chi$ = velocity potential at 750 mb

$Z = \nabla^2 \psi$

$ZTO = \nabla^2 \tau$

$ZRK = \nabla^2 \chi$

Table A4: Catalog of subroutines.

Subroutines for transformations

In the following subroutines:
 MM indicates number of points in spectral space in the longitudinal direction
 NN indicates number of points in spectral space in the latitudinal direction
 NG indicates number of points in physical space in the longitudinal direction
 NK indicates number of points in physical space in the latitudinal direction

SUBROUTINE TR1 (XI,X,MM,NN,N6,NK)

TR1 transfers variables from physical to spectral space
    Input: XI(NG,NK) = values in physical space
    Output: X(MM,NN) = spectral coefficients

SUBROUTINE TR2(X,XI,MM,NN,N6,NK)

TR2 transfers variables from spectral to physical space
    Input: X(MM,NN) = spectral coefficients
    Output: XI(NG,NK) = values in physical space

SUBROUTINE GUASS (FMK,FMN,NK,MM,NN)

GUASS transforms variables of the latitude circles from the Fourier to
the spherical harmonic domain
    Input: FMK(MM,NK) = Fourier coefficients
    Output: FMN(MM,NN) = spherical harmonics coefficients

SUBROUTINE RM1(X,K,MM,NN,XM)

RM1 for given latitude finds Fourier coefficient X(MM) for variable in
physical space
    Input: X(MM,NN) = variable in spherical harmonic domain
          K = index of latitude
    Output: XM(MM) = Fourier coefficients

SUBROUTINE RM2(X,K,NN,X,MM)

RM2 finds Fourier coefficients of the meridional derivative for variable
X on given latitude
    Input: X(MM,NN) variable in spherical harmonic domain
    Output: XMM(MM) = Fourier coefficient of meridional derivative of X

SUBROUTINE FFT991(A,WORK,TRIGS,IFAX,INC,JUMP,N,M,ISIPN)

FFT991 performs a number of simultaneous real/half-complex Fourier transforms,
or corresponding inverse transforms. See catalog of NCAR subroutines
(CRAYLIB library).

Subroutines for physical processes

SUBROUTINE SOLA (NK,ND)

SOLA calculates solar radiation absorbed by the earth and atmosphere.
Input: NK = number of gaussian latitudes
          ND = day of year
Output: QSE = solar radiation absorbed by the earth   } in COMMON/SRENG/
          QSR = solar radiation absorbed by atmosphere }

SUBROUTINE OROG(X,TO,ETA,XO,MM,NG,NK,ALPH)

OROG calculates velocity potential at the surface.
Input: X(MM,NN) = stream function harmonics
          TO(MM,NN) = shear harmonics
          ETA(MM,NN) = surface pressure divided by pressure increment
                    harmonics
          ALPH = parameters regulating height of topography
Output: XO(MM,NN) = surface velocity potential harmonics
          F24(NG,NK) = laplacian of surface velocity potential
          F25(NG,NK) = meridional derivative of surface velocity potential
          F26(NG,NK) = zonal derivative of surface velocity potential

SUBROUTINE ADTO (RK,COR,MM,NN)

ADTO calculates coriolis term with velocity potential
Input: RK(MM,NN) = velocity potential
Output: COR(MM,NN) = $\nabla(f\nabla\chi)$

FUNCTION EVAP(QS,QL1,V1,DRAG)

EVAP calculates evaporation from surface to the lower layer
Input: QS = saturation mixing ratio for surface temperature
          QL1 = saturation mixing ratio in the lower layer of atmosphere
          V1 = wind speed in the lower layer of atmosphere
          DRAG = drag coefficient

SUBROUTINE SURFT(PT1,Q1,V1,K,PTS,QS,CD,CW,EMS,SFE)

SURFT calculates surface temperature and saturation mixing ratio for this
temperature
Input: PT1 = air temperature at 1000 mb
          Q1 = relative humidity in the lower layer x saturated mixing
                  ratio for PT1
          V1 = wind speed in the lower layer
          K = latitude index
          PTS = surface temperature from previous time step
          CD = drag coefficient
          CW = wetness parameter
          EMS = surface emissivity of the earth
          SFE = parameter used in calculations of longwave emissivity
                  depending on cloud fraction and mixing ratio near the
                  surface
          QSE = solar radiation absorbed by the earth
          QSR = solar radiation absorbed by atmosphere
Output: PTS = surface temperature
          QS = mixing ratio for temperature PTS

FUNCTION SNLT (PTS,PTLS,V1,DRAG)

SNLT calculates sensible heat flux from the ground to the lower layer of atmosphere

Input: PTS = surface temperature
PTLS = temperature of the air at 1000 mb
V1 = wind speed in the lower layer
DRAG = drag coefficient

FUNCTION FLON (PTS,K)

FLON calculates clear sky outgoing radiation at the top of the atmosphere

Input: PTS = surface air temperature
RH = vertical mean relative humidity (in COMMON/RHLM/
K = index of latitude

SUBROUTINE TIME (X,TO,PT,SI,Q,MM,DT,NTIME)

TIME makes time step with smoothing

Input: RHS of eq. 4.7-4.11 (in COMMON/RHS/)
values of variables from N-1 time step (in COMMON/TIMES/)
DT = time step
NTIME = number of time step
MM = max wave number +1

Output: Values of variables on N+1 time step
X = stream function
TO = shear
PT = potential temperature
SI = static stability
Q = water vapor mixing ratio

SUBROUTINE BAL(PT,TO,MM,NN,τ)

BAL calculates shear τ from linear balance equation

Input: PT(MM,NN) = potential temperature
TO(1,NN) = shear calculated in subroutine TIME

Output: TO(MM,NN) = shear satisfying linear balance

SUBROUTINE SITER(RK,ZRK,RTO,RPT,GS1,SI,MM,NG,NK)

SITER solves equation for velocity potential χ in spherical harmonic domain

Input: RK(MM,NN) = velocity potential from previous time step
ZRK(MM,NN) = leplacian of velocity potential
RTO(MM,NN) = R.H.S. of equation for τ but without terms
containing velocity potential
RPT(MM,NN) = R.H.S. of equation for θ but without terms
containing χ
SI(MM,NN) = static stability

Output: RK(MM,NN) = new value of velocity potential
ZRK(MM,NN) = new value of $\nabla^2 \chi$
GS1(MM,NN) = velocity potential term in equation for θ
F13(NG,NK) = meridional derivative of χ
F14(NG,NK) = zonal derivative of χ
F20(NG,NK) = $\nabla^2 \chi$

SUBROUTINE ZAV(RTT,NG,NK,AV)

ZAV calculates zonal average of variable RTT
   Input: RTT(NG,KK) = variable in physical space
   Output: AV(NK) = zonal average of RTT

SUBROUTINE CONVEC(QG,PTG,SIG,PRCP,NG,NK,TIM)

CONVEC makes convective adjustment and calculates precipitation rate
   Input: QG(NG,NK) = mixing ratio before convective adjustment
            PTG(NG,NK) = potential temperature at 500 mb before convective
                      adjustment
            SIG(NG,NK) = static stability before convective adjustment
            TIM = time step
   Output: PTG(NG,NK) = potential temperature at 500 mb after convective
                      adjustment
            SIG(NG,NK) = static stability after convective adjustment
            PRCP(NG,NK) = precipitation rate